

A computer-aided diagnosis system for breast cancer detection by using a curvelet transform

Nebi GEDİK,^{1*} Ayten ATASOY²

¹Department of Maritime Transportation and Management Engineering, Faculty of Marine Sciences, Karadeniz Technical University, Sürmene, 61600 Trabzon, Turkey

²Department of Electrical and Electronics Engineering, Faculty of Engineering, Karadeniz Technical University, 61080 Trabzon, Turkey

Received: 05.01.2012 • Accepted: 28.03.2012 • Published Online: 03.06.2013 • Printed: 24.06.2013

Abstract: The most common type of cancer among women worldwide is breast cancer. Early detection of breast cancer is very important to reduce the fatality rate. For the hundreds of mammographic images scanned by a radiologist, only a few are cancerous. While detecting abnormalities, some of them may be missed, as the detection of suspicious and abnormal images is a recurrent mission that causes fatigue and eyestrain. In this paper, a computer-aided diagnosis system using the curvelet transform (CT) algorithm is proposed for interpreting mammograms to improve the decision making. The purpose of this study is to develop a method for the characterization of the mammography as both normal and abnormal regions, and to determine its diagnostic performance to differentiate between malignant and benign ones. The multiresolution CT that was recently derived is used to differentiate among 200 mammograms: 50 malignant, 50 benign, and 100 normal. A support vector machine and the k-nearest neighbor algorithm are used as classifiers to build the diagnostic model and are also used for the principal component analysis and linear discriminant analysis for further dimensional reduction and feature selection. A dataset from the Mammographic Image Analysis Society database is used for testing the method.

Key words: Mammography, computer-aided diagnosis, curvelet transform, linear discriminant analysis, principal component analysis, support vector machine, k-nearest neighbor

1. Introduction

One of the most dangerous types of cancer among women worldwide is breast cancer. Over 11% of women get this disease during their life. The World Health Organization's International Agency for Research on Cancer forecasts that there will be more than 1,000,000 patients with breast cancer worldwide and over 400,000 women will die due to breast cancer each year [1]. In breast cancer cases, early detection is important to reduce the fatality rate [2]. On the other hand, the early detection of breast cancer is not easy. Biopsy is applied for the most accurate diagnosis. However, it is an aggressive and high-cost procedure with some risk and causes inconvenience to the patient. Mammography is the best available inspection facility to detect the symptoms of breast cancer at the early stage and it can disclose information about abnormality, such as masses, microcalcifications, bilateral asymmetry, and architectural distortion. Mammography is the breast image taken with a special X-ray. It uses a low-dose X-ray, high-contrast, and high-resolution film [3].

For the hundreds of mammographic images scanned by a radiologist, only a few are cancerous. While

*Correspondence: ngedik@ktu.edu.tr

detecting abnormalities, some of them may be missed, as the detection of suspicious and abnormal images is a recurrent mission that causes fatigue and eyestrain. Therefore, computer-aided diagnosis (CAD) systems have been composed to assist radiologists in the determination of abnormalities in mammography. These systems are developed only as a second opinion and the final decision belongs to the radiologist. The systems have improved the radiologists' performance to achieve the best accuracy of breast cancer detection [4]. In this case, several algorithms have been proposed in the literature for CAD systems, for instance, directional filtering with Gabor wavelets [5], fractal modeling [6], independent component analysis [7,8], and efficient coding and linear discriminant analysis (LDA) [9].

The extraction of features is an important step that affects the classification process in pattern recognition and CAD systems. Features in the digital images can be obtained from the spatial data or a different space. Different space modalities use a transform such as Fourier, contourlet, wavelet, or curvelet transform (CT). Multiresolution tools such as these allow for the conservation of an image according to a certain level of resolution. They also allow zooming in the image. Multiresolution analysis is useful in many applications in image processing [10,11]. In this direction, several systems based on wavelet transform have been developed. Liu et al. [12] demonstrated that multiresolution analysis of mammographic images improves the effectiveness of wavelet-based CAD systems. A set of statistical features was used as the features and then a binary tree classifier was used to detect the speculated mass. The success rate of the classification obtained was 84.2%. Ceylan et al. [13] presented a new approach to medical image segmentation using the wavelet and neural network. They suggested a cascade method occurring from a complex-valued feature extractor, complex wavelet transform (CWT), and complex-valued classifier, the complex-valued artificial neural network (CVANN). They used the image from computed tomography to evaluate their cascade method. CVANN, using CWT, is applied to extract the lung area from a tomographic image. The size of the dataset that is input for the cascade technique is reduced using the complex discrete wavelet transform. The wavelet transform is applied at 1, 2, 3, and 4 grades. Inverse CWT is performed to get a segmented image.

Yang et al. [14] presented a comparative study to detect microcalcification from mammographic images via wavelet transform. Each image is decomposed into different resolution levels by using wavelet transform. Several normal wavelet functions were applied to a dataset and compared with each other. Different resolution levels were explored to detect the microcalcification for each wavelet function. They achieved the best detecting results using the Daubechies wavelet with fourth level decomposition. Rashed et al. [15] proposed a multiresolution mammogram analysis using wavelet transform. In that paper, Daubechies -4 , -8 , and -16 wavelets with 4 decomposition grades were used. Their feature vector was built using the biggest wavelet coefficients from each image. The classification success rate achieved was 87.06%. Ferreira et al. [16] worked on the origination and validation of a supervised classifier. They classified mammogram images using this classifier in 2 different approaches: as radial, circumscribed, microcalcifications, and normal mammograms; and as benign, malign, and normal ones. The feature vector was built with a different number of wavelet coefficients. They concluded that the results were very promising. Moayedi et al. [17] presented a study to detect masses in a digital mammogram using contourlet and support vector machine (SVM). In their study, the feature vector was generated from contourlet coefficients from the fourth decomposition grade, cooccurrence matrix, and geometrical features. In addition, a genetic algorithm was used for the feature selection and a neural network classifier was used in the classification stage. They concluded that the contourlet transform offers an improvement for the classification.

Candès et al. [18] developed a CT to provide a powerful representation of objects with discontinuities throughout their curves. It is very important to detect and to enhance the boundaries between different

structures in medical image processing [19]. Several studies using CTs have been done. CTs are used by researchers in image processing. Ali et al. [20] reported a CT approach for the fusion of magnetic resonance and computed tomography. The CT provided good results in their fusion experimentation. Eltoukhy et al. [21] presented an approach for the diagnosis of breast cancer via CT. Their feature vector included the biggest coefficients from CT. They selected a ratio (10%:90%) of features for every image and they classified the selected part using the Euclidean distance classifier. They used 142 mammogram images from the Mammographic Image Analysis Society (MIAS) dataset.

Murtagh et al. [22] presented a study that includes wavelet and curvelet moments for classification. They use 2nd, 3rd, and 4th order moments of transform coefficients as features. They also used the k-nearest neighbor (k-NN) algorithm as a classifier. Eltoukhy et al. [23] introduced a study of mammogram classification based on CT. They decomposed each image into different scales and angles. They selected a different ratio from biggest coefficients to use as the feature vector and they used a different decomposition level to detect the scale that provides the maximum classification accuracy. The maximum success rate was obtained at 98.59% for the normal and abnormal classification at scale 2 with 40% of the biggest coefficients, and at scale 3 with 40% and 70% of the biggest coefficients. Their comparative study with wavelet showed that the curvelet-based features yield a greater classification success rate than the wavelet-based features. Dehghani et al. [24] proposed a system based on texture feature extraction and SVM. Feature extraction is done using the statistical method and signal processing method from the regions of interest (ROI). The system used a new classifier based on SVM called weighted SVM. They compared the features from the cooccurrence matrix, wavelet transform, contourlet transform and contourlet plus cooccurrence matrix using SVM and weighted SVM. Eltoukhy et al. [25] presented another method for breast cancer diagnosis. They developed a feature extraction technique based on the statistical t-test method. The method builds a matrix that is created from vectors of wavelet or CT coefficients. After that, a dynamic threshold is implemented to get the most important features. The dataset is divided into training and testing data. For the classification stage, they used SVM as a classifier. The dataset was classified as normal and abnormal, and benign and malignant. The technique was repeated until achieving the best classification success with the least coefficients.

In this study, each mammogram image is decomposed into subbands using CT (at scale 3 and angle 8). Eltoukhy et al. [23] achieved a maximum success rate of 98.59% for normal and abnormal classification at scale 2 with 40% of the biggest coefficients, and at scale 3 with 40% and 70% of the biggest coefficients. Therefore, scale 3 is the scale chosen in this paper, because it yielded the most successful results in 2 previous studies. In contrast to Eltoukhy et al. [21,23,25], we focused on the approximation subband. A set of the approximation coefficients of each mammogram is extracted and the approximation coefficients are used to build the feature vector and the feature matrix. Next, principal component analysis (PCA) and LDA are applied to the coefficient matrix. The k-NN classifier and SVM are used to classify the mammographic dataset. The system proposed here consists of 2 main steps: the 1st step is to separate the normal and abnormal mammograms and the 2nd step is to classify the benign and malignant abnormal ones.

The remainder of the paper is organized as follows. Section 2 gives a brief introduction and the application steps of the CT, experimental work, and dataset from the MIAS. In Section 3, the results and discussion are presented. Section 4 contains the conclusions.

2. Description of the study

2.1. Curvelet transform

Candès and Donoho developed CT in 1999. Its development is based on image analysis needs [26]. The transform has a better skill of representing the edges and other singularities along curves in the image according to other multiresolution transforms. It also has better directional capability. A new design of CT was introduced in 2006 [27]. The new CT is faster, simpler, and easier to understand. The new CT is a multiscale and multidirectional transform that provides a better representation of the objects with edges. It also involves coefficients to represent the curves. To perform the CT, first, a 2-dimensional (2D) fast Fourier transform (FFT) of the image is taken. After that, the 2D Fourier frequency plane is divided into wedges. The wedges have a parabolic shape as a consequence of dividing the Fourier plane into radial and angular partitions. Finally, inverse FFT is applied to each wedge to find the curvelet coefficients. Figure 1 (on the left side) denotes the section of wedges of the Fourier frequency plane. Concentric circles (radial division) are responsible for decomposing the image into multiple scales and angular partitions corresponding to different angles. Because of this, addressing the particular wedge is necessary to determine the angle and the scale at first. Each wedge corresponds to a particular curvelet according to a specific scale and angle in the spatial domain. Figure 1 (on the right side) denotes curvelets in a spatial cartesian grid at a particular scale and angle. Fast digital CT (FDCT) redesigned has 2 different digital applications [27]: curvelets by way of unequally spaced FFT and curvelets by way of wrapping. For detailed FDCT information, and its implementation, one can refer to [27].

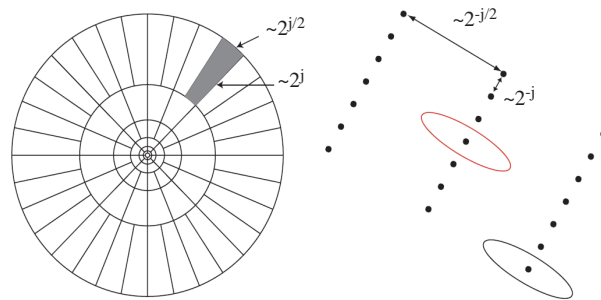


Figure 1. Curvelets for Fourier frequency on the left side and spatial domain on the right side.

The curvelets via wrapping are described below with the basic steps [27]:

Step 1: Compute 2D FFT coefficients to obtain Fourier samples $\hat{f}[n_1, n_2]$.

Step 2: Interpolation, for each scale and angle pair (j, l) , $\tilde{U}_{j,l}[n_1, n_2] \hat{f}[n_1, n_2]$.

Step 3: Wrap result of step 2 around the origin and obtain $\tilde{f}_{j,l}[n_1, n_2] = W(\tilde{U}_{j,l} \hat{f})[n_1, n_2]$, where the range n_1 and n_2 are $0 \leq n_1 \leq L_{1,j}$ and, $0 \leq n_2 \leq L_{2,j}$ respectively.

Step 4: Implement the inverse 2D FFT for each $\tilde{f}_{j,l}$ to obtain the discrete coefficients.

The Fourier frequency plane of each image is split into radial and angular wedges in the first 2 steps, because there is a parabolic relationship between the length and width of the curvelet in Figure 1. Each generated wedge corresponds to curvelet coefficients at a given scale and angle pair. The data are reindexed around the origin in step 3. Figures 2a and 2b illustrate the original and warped segments around the origin, respectively. Finally, inverse FFT is implemented to get the curvelet coefficients in the spatial domain [27].

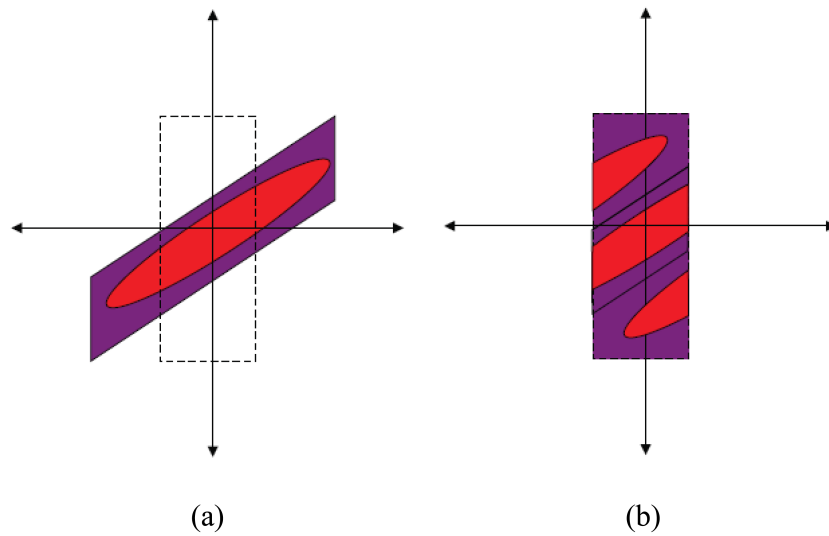


Figure 2. a) Original segment and b) wrapped segment around the origin [28].

2.2. Experimental work

The system proposed in this paper is based on a multiresolution representation of the mammographic images using a curvelet. CT at scale 3 and angle 8 is implemented to decompose the images into curvelet subbands. As a result of the application, 25 components are produced. One of them is an approximate subband and the other ones are detailed subbands. This study is focused on the approximate subband. Approximate coefficients from each image are used to create the feature matrix. The classification process is performed both with and without PCA and LDA using a k-NN classifier and SVM.

PCA and LDA are useful statistical techniques used in image processing. PCA covers standard deviation, covariance, eigenvectors, and eigenvalues [29]. A multidimensional interrelated dataset is transformed to be a much lower dimensional dataset by keeping as much information as possible in PCA. The original data are transformed into a series of uncorrelated principal components (PCs). In the series of PCs, data are ordered from high variance to low variance, where the first few PCs can contain the most information. LDA attempts to find directions that maximize separability between the datasets [30]. The method maximizes the proportion between-class variance and the within-class variance for any data. The aim is to provide the maximum separability. The main dissimilarity between LDA and PCA is that when the original data have been transferred to a different space, their shape and location change in PCA. The location is invariable in LDA. It makes an effort to ensure more class separability and draw a decision area between the given classes. This method also ensures that the distribution of the feature data is more understandable.

In this study, a dataset that is supplied by the MIAS [31] is used to apply the proposed method. At the MIAS, images were examined and labeled by an expert radiologist. This database contains a file description list belonging to the mammograms and provides the appropriate details about each image. Some of these details are the class of the abnormality, (x, y) coordinates of an abnormality according to its center, and the approximate radius (in pixels) of a circle that is surrounded by an abnormality. The reason that the details are required is that the dataset includes various cases. This database is also commonly used in similar research.

We chose 200 mammogram images, including 50 malignant, 50 benign, and 100 normal, in this study. A ROI that contains the lesion in the cases of the benign and malignant mammograms is manually selected for

each mammogram. ROI are found according to the (x, y) coordinates of the center of the abnormality, where the coordinates are given in the file list of the MIAS database. Therefore, almost all the background information and most of the noise are eliminated. The ROI of the normal mammograms are randomly selected. Only the pectoral muscle is not taken into account as a possible ROI. Due to the fact that tissues have different sizes, different pixel values for every subband are chosen and the mammograms are resized to 24×24 , 50×50 , and 200×200 pixels. The subband that has 200×200 pixels involves the largest mass. An example of cropping and the basic block diagram of the proposed diagnosis system are given in Figure 3.

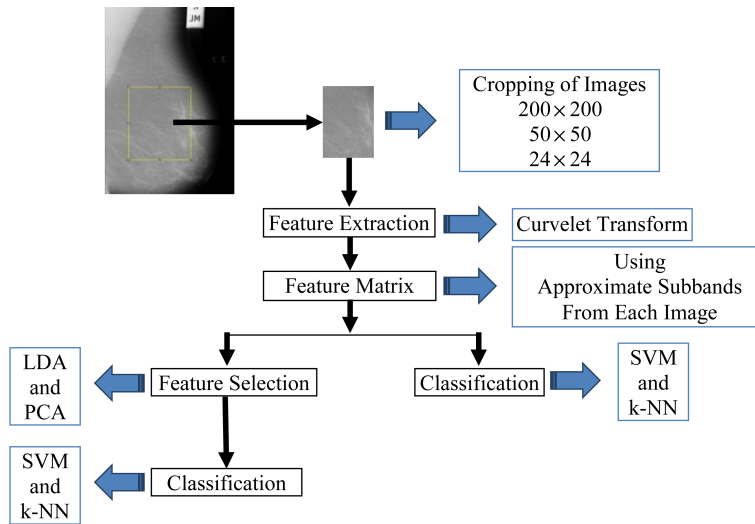


Figure 3. The system proposed for mammogram diagnosis.

The CT is applied at scale 3 and angle 8 after the mammograms are cropped as described. Figure 4 justifies our approach of selecting only 1 subband by showing the approximate and detailed subbands for scale 3 and angle 8. The feature vectors are built from approximate coefficients for each image. It is noticeable that the approximate subband has the maximum standard deviation among the curvelet subbands. The feature matrix is obtained from the feature vectors for the classification stage. In this stage, the SVM and k-NN classifiers are

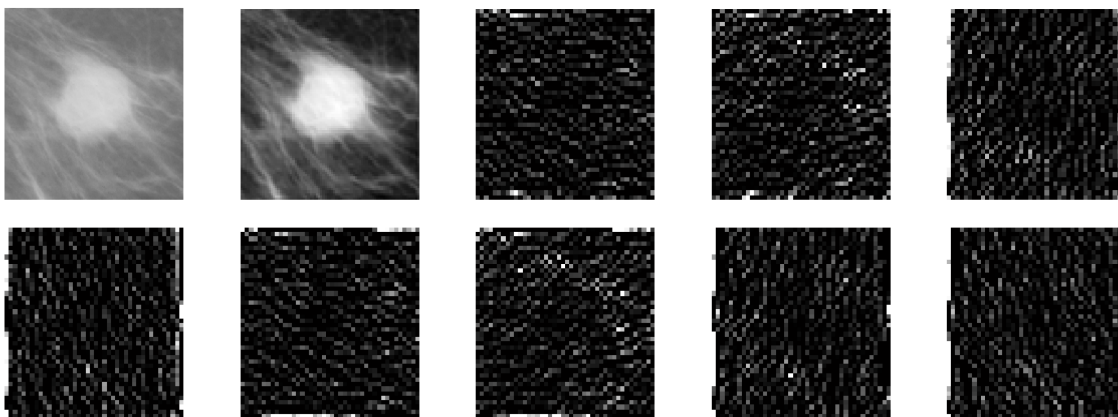


Figure 4. The 1st one is the original image from the MIAS database, mdb028, the 2nd one is the approximate subband, and the others are detailed subbands at angle 8.

applied to the training and testing feature matrices, both with and without PCA and LDA. PCA and LDA are applied on these feature matrices to reduce the dimensionality further and to select the features. The optimum k values were investigated using various k values from 1 to 30 on every stage using the k-NN classifier. The optimum results were obtained by different k values.

3. Results and discussion

All of the classification applications in this paper are done for 200×200 , 50×50 , and 24×24 pixels of mammogram images. In the first step of this work, the dataset is classified as normal and abnormal. The dataset is divided into a sample in 200 ROI: 100 for training and 100 for testing. The training set has 50 abnormal and 50 normal mammogram samples. The testing set also has 50 abnormal and 50 normal mammogram samples. Table 1 shows comparatively the success rates for the classification of the mammogram images as normal and abnormal via CT without LDA and CT with LDA. Table 2 shows the success rates of the classification as normal and abnormal via CT with PCA for the same application using different components.

After that, the sensitivity and specificity analyses are done for the same data. For this purpose, the following expressions are used:

$$\text{Sensitivity} = \frac{TP}{TP + FN} (\%), \quad (1)$$

$$\text{Specificity} = \frac{TN}{FP + TN} (\%), \quad (2)$$

where TP, TN, FP, and FN indicate the true positives, true negatives, false positives, and false negatives, respectively.

The values of sensitivity and specificity obtained using CT, with and without LDA, for a 50%–50% training-test partition are shown in Table 1. Figures 5a and 5b illustrate the receiver operating characteristic (ROC) curves to show the effectiveness of each classifier by using CT without LDA. Figures 6a and 6b illustrate the ROC curves to show the effectiveness of each classifier using CT with LDA.

Table 1. The success rates and sensitivity and specificity values for the classification of the mammogram images as normal and abnormal via CT without and with LDA.

Pixels	CT			CT + LDA			Classifier	k Values	
	Success rates (%)	Sensitivity (%)	Specificity (%)	Success rates (%)	Sensitivity (%)	Specificity (%)		CT	CT + LDA
200×200	87	80	94	100	100	100	SVM		
	81	70	92	100	100	100	k-NN	3	3
50×50	85	82	88	100	100	100	SVM		
	80	78	82	100	100	100	k-NN	3	3
24×24	82	82	82	93	92	94	SVM		
	77	84	70	97	94	100	k-NN	7	17

The second step has the task of classifying the abnormal mammogram images as malignant and benign, as it has already shown the classification of the abnormal and normal regions with great accuracy. In this direction, 100 abnormal regions from the MIAS database are used, which are divided into 50 malignant and 50 benign regions. For the training procedure, 25 malignant and 25 benign regions are used, while the remaining 25 malignant and 25 benign regions serve for the evaluation of the system. Table 3 shows comparatively the success rates for the classification of the abnormal mammogram images as malignant and benign via CT with and without LDA. Table 4 shows the success rates for the classification of the mammogram images as malignant and benign via CT with PCA.

Table 2. The success rates for the classification of the mammogram images as normal and abnormal via CT and PCA for the 50%–50% training-test partition.

CT + PCA	Success rates (%)			Classifier	k Values		
	200 × 200	50 × 50	24 × 24		200 × 200	50 × 50	24 × 24
3 comp.	90	90	83	SVM			
	81	81	78	k-NN	3	3	7
6 comp.	90	83	90	SVM			
	79	77	78	k-NN	3	3	7
9 comp.	85	88	95	SVM			
	86	80	77	k-NN	3	3	7
12 comp.	85	88	81	SVM			
	86	80	77	k-NN	3	3	7
30 comp.	88	85	70	SVM			
	81	80	77	k-NN	3	3	7
50 comp.	86	85	61	SVM			
	83	80	77	k-NN	3	3	7

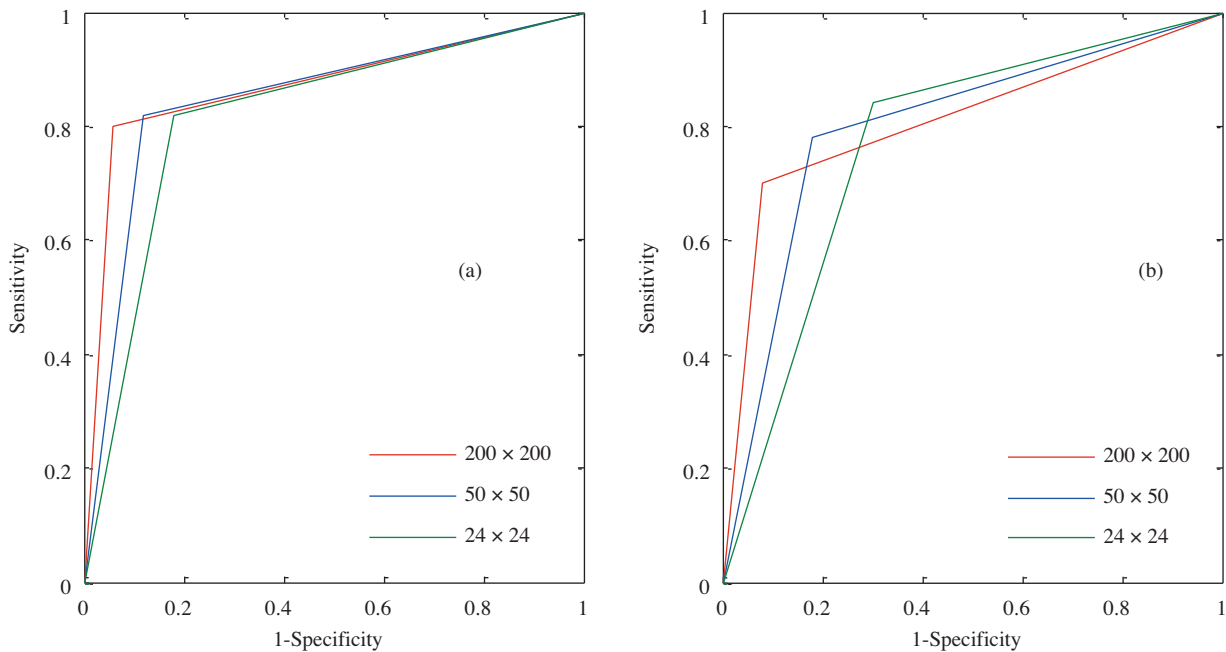


Figure 5. ROC curves for the normal-abnormal separation based on CT: a) for the SVM classifier and b) for the k-NN classifier.

After that, the sensitivity and specificity analysis is also done for the second step. The values of sensitivity and specificity for separating the mammogram images as malignant and benign using CT with and without LDA are shown in Table 3. Figures 7a and 7b illustrate the ROC curves of each classifier via CT without LDA. Figures 8a and 8b illustrate the ROC curves of each classifier via CT with LDA.

In the third step of this work, a 5-fold cross validation is used to examine the classification accuracy of these algorithms for the normal-abnormal separating task. This step has 2 sections. In first section, the dataset is classified as normal and abnormal. Hence, the dataset is partitioned into 5 different samples from 200 ROI: 100 normal and 100 abnormal mammogram images. While a different fold of the data is held-out for validation,

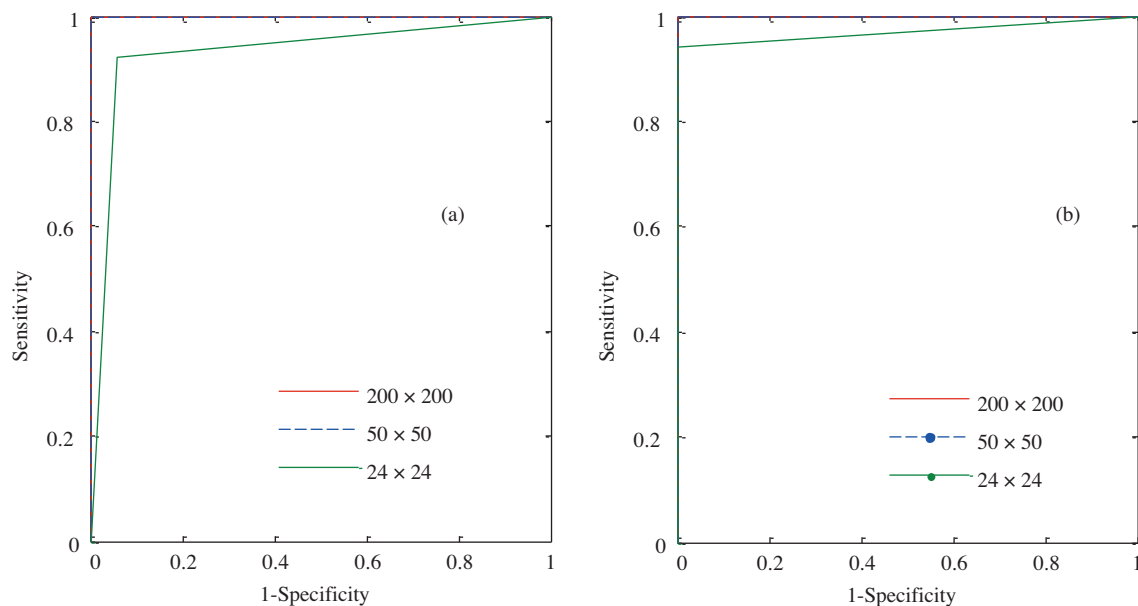


Figure 6. ROC curves for the normal-abnormal separation based on CT and LDA: a) for the SVM classifier and b) for the k-NN classifier.

Table 3. Classification success rates and sensitivity and specificity values for separating the mammogram images as malignant and benign via CT without and with LDA.

Pixels	CT			CT + LDA			Classifier	k Values	
	Success rates (%)	Sensitivity (%)	Specificity (%)	Success rates (%)	Sensitivity (%)	Specificity (%)		CT	CT + LDA
200 × 200	48	48	48	98	100	96	SVM		
	58	72	44	98	100	96	k-NN	3	3
50 × 50	42	52	32	92	92	92	SVM		
	54	44	64	92	96	88	k-NN	29	9
24 × 24	48	52	44	64	64	64	SVM		
	54	80	28	66	56	76	k-NN	7	7

Table 4. The success rates for classification of the mammogram images as malignant and benign via CT and PCA.

CT + PCA	Success rates (%)			Classifier	k Values		
	200 × 200	50 × 50	24 × 24		200 × 200	50 × 50	24 × 24
3 comp.	52	48	58	SVM			
	60	56	58	k-NN	13	17	3
6 comp.	56	54	52	SVM			
	58	54	56	k-NN	7	17	3
9 comp.	58	56	70	SVM			
	64	54	60	k-NN	13	17	3
12 comp.	50	60	72	SVM			
	58	54	60	k-NN	11	9	3
30 comp.	46	52	56	SVM			
	60	52	58	k-NN	25	9	3
50 comp.	42	52	56	SVM			
	60	52	58	k-NN	19	9	3

the remaining 4 folds are used for learning in each iteration. Table 5 shows the success rates in the classification of the mammogram images using CT without and with LDA, respectively.

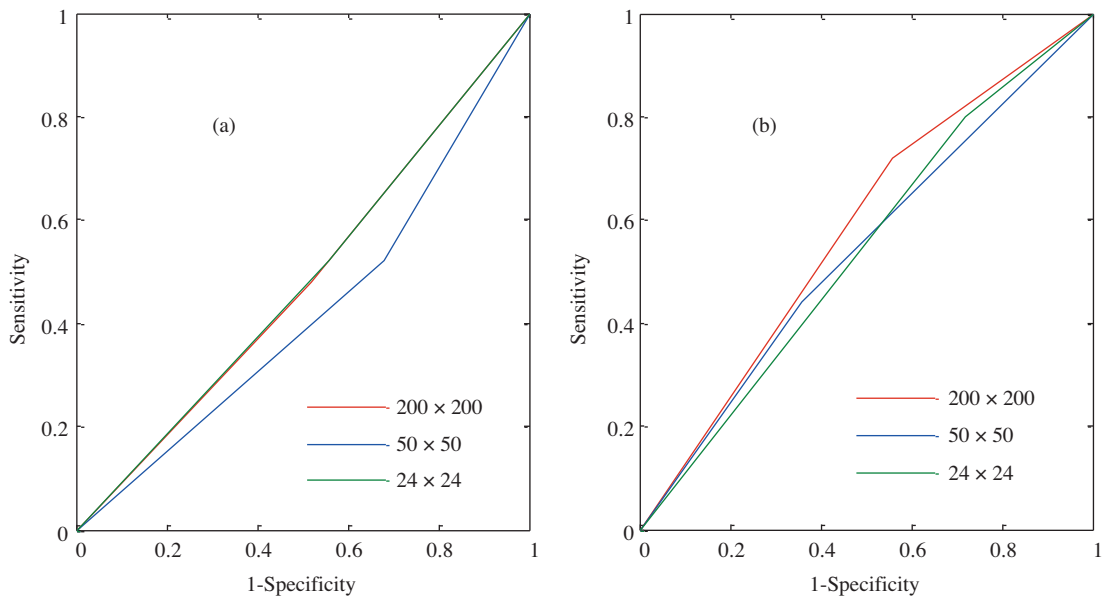


Figure 7. ROC curves for the malignant-benign separation based on CT: a) for the SVM classifier and b) for the k-NN classifier.

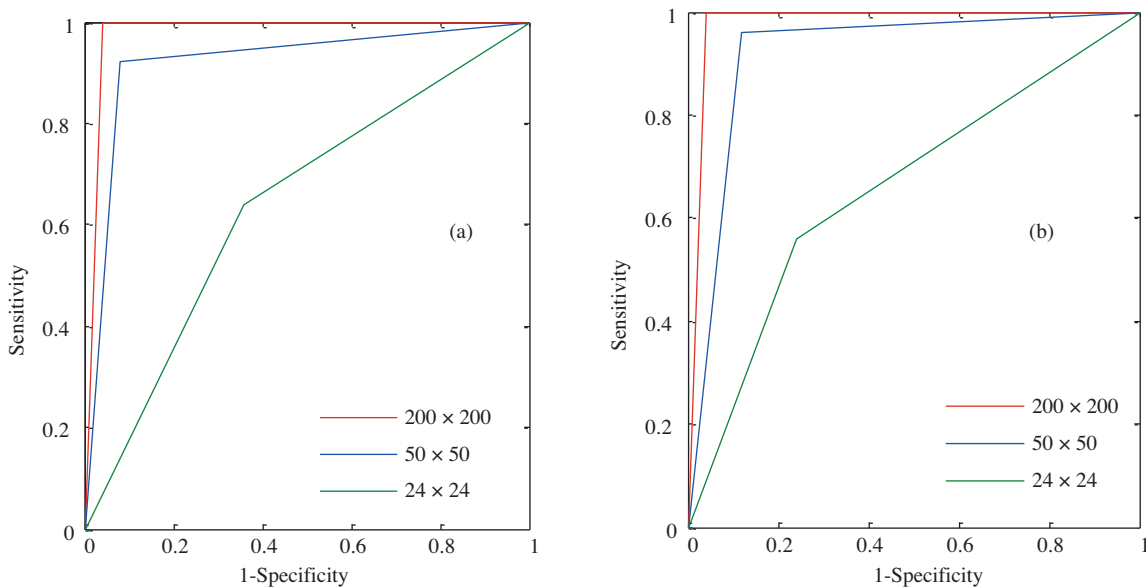


Figure 8. ROC curves for the malignant-benign separation based on CT and LDA: a) for the SVM classifier and b) for the k-NN classifier.

In the second section, the abnormal mammogram images are classified as malignant and benign with a 5-fold cross validation technique, as within normal and abnormal classification. Table 6 shows the success rates in the classification process as the malignant and benign abnormal mammogram images via CT without and with LDA for 5-fold cross validation, respectively.

Table 5. The success rates in the classification of the mammogram images as normal and abnormal for CT without and with LDA for 5-fold cross validation.

Pixels	Partition and success rates														Classifier
	Without LDA (%)					With LDA (%)					Average (%)				
	Fold1	Fold2	Fold3	Fold4	Fold5	Fold1	Fold2	Fold3	Fold4	Fold5	Without LDA	With LDA			
200 × 200	82.5	90	95	80	87.5	100	100	100	100	100	87	100	SVM		
	82.5	72.5	87.5	90	85	100	100	100	100	100	83.5	100	k-NN		
50 × 50	75	90	92.5	75	92.5	100	100	100	100	100	85	100	SVM		
	72.5	80	92.5	92.5	80	100	100	100	100	100	83.5	100	k-NN		
24 × 24	80	87.5	90	85	80	82.5	45	87.5	97.5	52.5	84.5	73	SVM		
	70	85	85	90	77.5	87.5	72.5	95	97.5	60	81.5	82.5	k-NN		

Table 6. The success rates for the separation as malignant and benign mammogram images using CT without and with LDA for 5-fold cross validation.

Pixels	Partition and success rates														Classifier
	Without LDA (%)					With LDA (%)					Average (%)				
	Fold1	Fold2	Fold3	Fold4	Fold5	Fold1	Fold2	Fold3	Fold4	Fold5	Without LDA	With LDA			
200 × 200	30	40	40	40	25	100	75	100	100	100	35	95	SVM		
	65	60	60	60	65	100	85	100	100	100	62	97	k-NN		
50 × 50	35	45	55	35	45	100	60	70	95	95	43	84	SVM		
	60	65	60	50	60	100	65	75	95	95	59	86	k-NN		
24 × 24	45	65	60	45	55	50	55	55	60	65	54	57	SVM		
	55	70	60	50	50	75	55	65	75	75	57	69	k-NN		

4. Conclusion

Breast cancer diagnosis using a digital mammogram is a practical field for medical application. The positive results that come from a CAD system affect the mortality rate of the patients. In this paper, we implement a CAD system and investigate the performance of the CT method in the problem of recognizing breast cancer in the ROI of digital mammograms. A different classification scheme is applied in the classification of breast cancer. The originality of the study is that the different features obtained by CT are used in the hybrid classification of breast cancer with the SVM, k-NN, PCA, and LDA algorithms. We obtain approximate curvelet coefficients from each image as the feature vector to be used for the classification. The presented results demonstrate that CT is a useful tool to discriminate malignant, benign, and normal tissues. Furthermore, the CT and LDA obtain the best performance for classifying the normal and abnormal mammograms, with a success rate of 100% in a dataset of 200×200 and 50×50 pixels for a 50%–50% training-test partition and a 5-fold cross validation. In addition, the system that combined the features obtained from the CT and LDA is capable of best classifying the ROI as benign or malignant with a recognition rate of 98% and 97% for the 50%–50% training-test partition and a 5-fold cross validation, respectively. For the CT and principle component analysis, the best performance of classifying the normal and abnormal mammograms is 95%, 90%, and 90% for the 50%–50% training-test partition in datasets of 24×24 , 50×50 , and 200×200 pixels, respectively. Based on these results, it is observed that such features provide significant support for more detailed clinical investigations and the results are very encouraging when tissues are classified with CT and LDA.

References

- [1] N.R. Pal, B. Bhowmick, S.K. Patel, S. Pal, J. Das, “A multi-stage neural network aided system for detection of micro-calcifications in digitized mammograms”, *Neurocomputing*, Vol. 71, pp. 2625–2634, 2008.
- [2] J.C. Fu, S.K. Lee, S.T.C. Wong, J.Y. Yeh, A.H. Wang, H.K. Wu, “Image segmentation, feature selection and pattern classification for mammographic microcalcifications”, *Computerized Medical Imaging and Graphics*, Vol. 29, pp. 419–29, 2005.
- [3] R.M. Rangayyan, F.J. Ayres, J.E.L. Desautels, “A review of computer aided diagnosis of breast cancer: toward the detection of subtle signs”, *Journal of the Franklin Institute*, Vol. 344, pp. 312–348, 2007.
- [4] M.L. Giger, N. Krassemeijer, S.G. Armato, “Computer aided diagnosis in medical imaging”, *IEEE Transactions on Medical Imaging*, Vol. 20, pp. 1205–1208, 2001.
- [5] R.J. Ferrari, R.M. Rangayyan, J.E.L. Desautels, A.F. Frere, “Analysis of asymmetry in mammograms via directional filtering with Gabor wavelets”, *IEEE Transactions on Medical Imaging*, Vol. 20, pp. 953–964, 2001.
- [6] L. Bocchi, G. Coppini, J. Nori, G. Valli, “Detection of single and clustered microcalcifications in mammograms using fractals models and neural networks”, *Medical Engineering and Physics*, Vol. 26, pp. 303–312, 2004.
- [7] I. Christoyianni, A. Koutras, E. Dermatas, G. Kokkinakis, “Computer aided diagnosis of breast cancer in digitized mammograms”, *Computerized Medical Imaging and Graphics*, Vol. 26, pp. 309–319, 2002.
- [8] F.A. Lúcio Campos, A.C. Silva, A.K. Barros, “Diagnosis of breast cancer in digital mammograms using independent component analysis and neural networks”, *Proceedings of the 10th Iberoamerican Congress conference on Progress in Pattern Recognition, Image Analysis and Applications*, Vol. 3773, pp. 460–469, 2005.
- [9] D.D. Costa, F. Lúcio Campos, A.K. Barros, “Classification of breast tissue in mammograms using efficient coding”, *Biomedical Engineering on Line*, Vol. 10, pp. 50, 2011.
- [10] S.G. Mallat, “A theory for multiresolution signal decomposition: the wavelet representation”, *IEEE Transactions on Pattern Analysis and Machine Intelligence*, Vol. 7, pp. 674–693, 1989.
- [11] R. Mousa, Q. Munib, A. Moussa, “Breast cancer diagnosis system based on wavelet analysis and fuzzy-neural”, *Expert Systems with Applications*, Vol. 28, pp. 713–723, 2005.

- [12] S. Liu, C.F. Babbs, E.J. Delp, “Multiresolution detection of speculated lesions in digital mammograms”, *IEEE Transactions on Image Processing*, Vol. 10, pp. 874–884, 2001.
- [13] M. Ceylan, Y. Özbay, N.O. Uçan, E. Yıldırım, “A novel method for lung segmentation on chest CT images: complex-valued artificial neural network with complex wavelet transform”, *Turkish Journal of Electrical Engineering & Computer Sciences*, Vol. 18, 2010.
- [14] J.C. Yang, J.W. Shin, D.S. Park, “Comparing study for detecting microcalcifications in digital mammogram using wavelets”, *Lecture Notes in Computer Science*, Vol. 3177, pp. 409–415, 2004.
- [15] E.A. Rashed, I.A. Ismail, S.I. Zaki, “Multiresolution mammogram analysis in multilevel decomposition”, *Pattern Recognition Letters*, Vol. 28, pp. 286–292, 2007.
- [16] C.B.R. Ferreira, D.L. Borges, “Analyses of mammogram classification using a wavelet transform decomposition”, *Pattern Recognition Letters*, Vol. 24, pp. 973–982, 2003.
- [17] F. Moayedi, Z. Azimifar, R. Boostani, S. Katebi, “Contourlet based mammography mass classification”, *Lecture Notes in Computer Science*, Vol. 4633, pp. 923–934, 2007.
- [18] E.J. Candès, D.L. Donoho, “Curvelets, multiresolution representation, and scaling laws”, *SPIE Wavelet Applications in Signal and Image Processing VIII*, Vol. 4119, 2000.
- [19] K.P. Soman, K.I. Ramachandran, “Insight Into Wavelets: From Theory to Practice”, 2nd ed., Prentice-Hall of India Pvt. Ltd., 2005.
- [20] F.E. Ali, I.M. El-Dokany, A.A. Saad, F.E. Abd El-Samie, “Curvelet fusion of MR and CT images”, *Progress in Electromagnetics Research*, Vol. 3, pp. 215–224, 2008.
- [21] M.M. Eltoukhy, I. Faye, B.B. Samir, “Using curvelet transform to detect breast cancer in digital mammogram”, *5th International Colloquium on Signal Processing and Its Applications*, pp. 340–345, 2009.
- [22] F. Murtagh, J. Starck, “Wavelet and curvelet moments for image classification: application to aggregate mixture grading”, *Pattern Recognition Letters*, Vol. 29, pp. 1557–1564, 2008.
- [23] M.M. Eltoukhy, I. Faye, B.B. Samir, “Breast cancer diagnosis in digital mammogram using multiscale curvelet transform”, *Computerized Medical Imaging and Graphics*, Vol. 34, pp. 269–276, 2010.
- [24] S. Dehghani, M.A. Dezfooli, “Breast cancer diagnosis system based on contourlet analysis and support vector machine”, *World Applied Sciences Journal*, Vol. 13 pp. 1067–1076, 2011.
- [25] M.M. Eltoukhy, I. Faye, B.B. Samir, “A statistical based feature extraction method for breast cancer diagnosis in digital mammogram using multiresolution representation”, *Computers in Biology and Medicine*, Vol. 42, pp. 123–128, 2012.
- [26] E.J. Candès, D.L. Donoho, “Curvelets: a surprisingly effective non-adaptive representation for objects with edges”, In: C. Rabut, A. Cohen, L.L. Schumaker, eds., *Curves and Surfaces*, Nashville, TN, Vanderbilt University Press, pp. 105–120, 2000.
- [27] E.J. Candès, L. Demanet, D.L. Donoho, L. Ying, “Fast discrete curvelet transform”, *SIAM Multiscale Modeling and Simulations*, Vol. 5, pp. 861–899, 2007.
- [28] Ericson B., “The very fast curvelet transform.ppt”, Available at: <http://homepages.cae.wisc.edu/~ece734/project/s06/eriksson.ppt>, 2012.
- [29] M.S. Nixon, A.S. Aguado, *Feature Extraction and Image Processing*, 2nd ed., Amsterdam, The Netherlands, Elsevier, 2008.
- [30] A.R. Webb, *Statistical Pattern Recognition*, 2nd ed., New York, Wiley, 2002.
- [31] MIAS Data Base Web Page, Available at: <http://peipa.essex.ac.uk/info/mias.html>, 2012.